ELSEVIER

Int. J. Therm. Sci. 41 (2002) 360–368

International Journal of Thermal Sciences

www.elsevier.com/locate/ijts

Laminar natural convection in inclined open shallow cavities

O. Polat, E. Bilgen [1,*]

École Polytechnique Box 6079, "City Center", Montréal, PQ, H3C 3A7, Canada

Received 5 December 2000; accepted 24 May 2001

Abstract

Laminar steady state natural convection in inclined shallow cavities has been numerically studied. The side facing the opening is heated by a constant heat flux, sides perpendicular to the heated side are insulated and the opening is in contact with a fluid at constant temperature and pressure. Equations of mass, momentum and energy are solved using constant properties and Boussinesq approximation and assuming an approximate boundary conditions at the opening. Isotherms and streamlines are produced, heat and mass transfer is calculated for Rayleigh numbers from 10^3 to 10^{10}, cavity aspect ratio $A = H/L$ from 1 to 0.125. The results show that flow and heat transfer are governed by Rayleigh number, aspect ratio and the inclination. Heat transfer approaches asymptotic values at Rayleigh numbers independent of the aspect ratio. The asymptotic values are close to that for a flat plate with constant heat flux. The effect of elongation of open cavities is to delay this asymptotic behavior. It is also found that the inclination angle of the heated plate is an important parameter affecting volumetric flow rate and the heat transfer.

Keywords: Natural convection; Convection in cavities; Inclined cavities; Heat transfer in natural convection

1. Introduction

Open cavities are encountered in various engineering systems, such as open cavity solar thermal receivers, uncovered flat plate solar collectors having rows of vertical strips, electronic chips, geothermal reservoirs, etc. Numerical studies on open cavities have been performed in simulating various applications. Representative studies may be categorized as side facing open cavities with an aspect ratio of one [1–3], inclined open cavities with an aspect ratio of the order of unity [4] and shallow cavities with small aspect ratio [5]. Similarly experimental studies have been performed using open cavities with an aspect ratio of one [6–8] and shallow cavities [9,10].

Le Quere et al. [1] investigated open isothermal square cavities using primitive variables. Penot [2] investigated the same configuration using stream function-vorticity formulation. Chan and Tien [3], on the other hand, performed a numerical study using SIMPLER algorithm on an open square cavity with isothermal heated side and adiabatic top and bottom walls. To overcome the difficulties of unknown conditions at the opening, these studies used an extended domain of computation. Later Chan and Tien [5] investigated open shallow cavity by using the same algorithm but restricting the computation to within the cavity. In comparing with their earlier study with open square cavity [3] and experimental study with open shallow cavity [9], they showed that for an aspect ratio of one, good heat transfer results could be obtained, particularly at high Rayleigh numbers. For shallow cavities, because of the far distance between the end boundaries, the results were even better. Mohamad [4] studied isothermal inclined open cavities with aspect ratio from 0.5 to 2 and showed that the inclination angle did not have any significant effect on the heat transfer rate from the isothermal bottom plate, but substantial one on the local Nusselt number. This aspect was also experimentally investigated by Cha and Choi [8] using an inclined open square cavity, which produced similar findings. Bilgen [10] reported an experimental study with side facing open cavities formed by vertical strips, which had an aspect ratio of about 0.4. The heated side was imposed a constant heat flux while the top and bottom walls were quasi-adiabatic. It was shown that in solar energy applications, the radiation heat exchange could be

* Correspondence and reprints.
E-mail address: bilgen@polymtl.ca (E. Bilgen).
[1] Present address: Shizuoka University, Faculty of Engineering, Hamamatsu, Japan.

1290-0729/02/$ – see front matter
PII: S1290-0729(02)01326-1

Nomenclature

A	enclosure aspect ratio $= H/L$
c_p	heat capacity ..... $J{\cdot}kg^{-1}{\cdot}K^{-1}$
g	acceleration due to gravity ..... $m{\cdot}s^{-2}$
H	cavity height ..... m
k	thermal conductivity ..... $W{\cdot}m^{-1}{\cdot}K^{-1}$
L	cavity width ..... m
Nu	Nusselt number $= hL/k$
p	pressure ..... Pa
P	dimensionless pressure $= (p - p_\infty)L^2/\rho\alpha^2$
Pr	Prandtl number $= \nu/\alpha$
q''	heat flux ..... $W{\cdot}m^{-2}{\cdot}K^{-1}$
q	dimensionless heat flux $= \frac{\partial T}{\partial X}$
Ra	Rayleigh number $= g\beta q'' L^4/(\nu\alpha k)$
T	dimensionless temperature $= (T' - T'_\infty)/(Lq''/k)$
U, V	dimensionless fluid velocities $= uL/\alpha, vL/\alpha$
$\dot{V}$	dimensionless volume flow rate through the opening
X, Y	dimensionless Cartesian coordinates $= x/L,\ y/L$
x, y	Cartesian coordinates

Greek symbols

α	thermal diffusivity ..... $m^2{\cdot}s^{-1}$
β	volumetric coefficient of thermal expansion ..... $1{\cdot}K^{-1}$
ν	kinematic viscosity ..... $m^2{\cdot}s^{-1}$
ρ	fluid density ..... $kg{\cdot}m^{-3}$
ψ	stream function
φ	inclination angle of the heated wall from the horizontal ..... °

Superscripts

$'$	dimensional variables
$-$	average

Subscripts

a	air
loc	local value
in	into cavity
max	maximum
min	minimum
out	out of cavity
∞	ambient value

non-negligible and also natural convection in open cavities heated by a constant heat flux should be addressed excluding and including the radiation effect.

The aim of this study is to examine the laminar natural convection in two-dimensional inclined open cavities. The side facing the opening is imposed by a constant heat flux while the other sides perpendicular to the heated wall are adiabatic. It is seen from the literature review that the case with constant heat flux imposed on the side wall of inclined shallow open cavities has not been addressed.

2. Problem description

In applications such as flat plate solar collectors and electronic chips where small open cavities are formed, the order of magnitude of cavity dimensions is usually small and the temperature difference created by the heat flux is not high. Therefore the heat transfer is dominated by laminar natural convection. Often small cavities are formed using fins, which are quasi adiabatic due to symmetry. A schematic of the two-dimensional system with geometrical and boundary conditions is shown in Fig. 1(a). Constant heat flux, q'' is applied on the wall facing the opening and transfered by natural convection to a fluid circulating through the right opening to the ambient or a fluid reservoir at a characteristic temperature T'_∞. Other two boundaries of the open cavity are adiabatic.

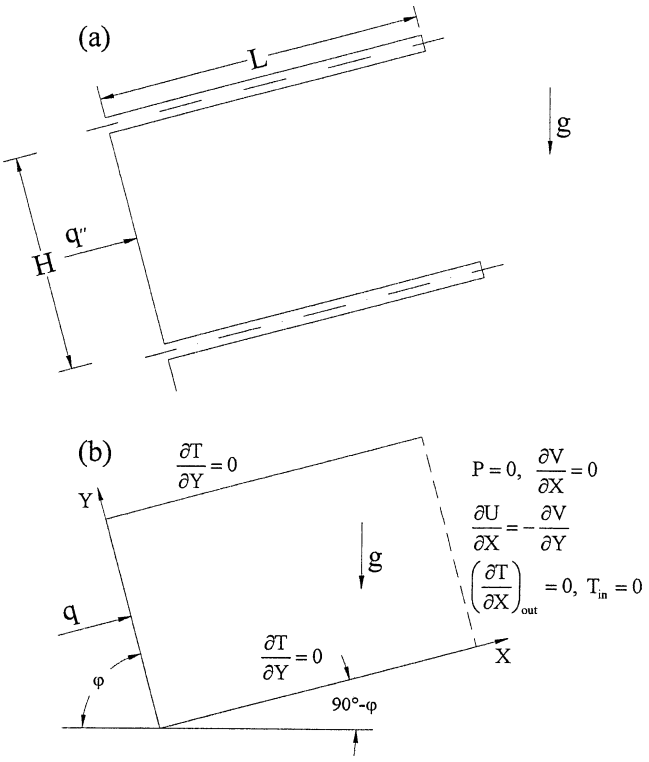

Fig. 1. (a) Schematic of open shallow cavity; (b) Coordinate system and boundary conditions.

3. Mathematical model

The continuity, momentum and energy equations for a two-dimensional laminar flow of an incompressible Newtonian fluid are written. Following assumptions are made: there is no viscous dissipation, the gravity acts in the vertical direction, fluid properties are constant and fluid density variations are neglected except in the buoyancy term (the Boussinesq approximation) and radiation heat exchange is negligible. Using non-dimensional variables defined in the nomenclature, the non-dimensional governing equations are obtained as

$$\frac{\partial U}{\partial X}+\frac{\partial V}{\partial Y}=0 \tag{1}$$

$$U\frac{\partial U}{\partial X}+V\frac{\partial U}{\partial Y}=-\frac{\partial P}{\partial X}+Ra\,Pr\,T\cos\varphi+Pr\,\nabla^2 U \tag{2}$$

$$U\frac{\partial V}{\partial X}+V\frac{\partial V}{\partial Y}=-\frac{\partial P}{\partial Y}+Ra\,Pr\,T\sin\varphi+Pr\,\nabla^2 V \tag{3}$$

$$U\frac{\partial T}{\partial X}+V\frac{\partial T}{\partial Y}=\nabla^2 T \tag{4}$$

The local, average and normalized Nusselt numbers are calculated respectively as

$$\begin{cases} Nu_{\mathrm{loc}}=-\dfrac{1}{T} \\ \overline{Nu}=\dfrac{1}{A}\displaystyle\int_0^A Nu_{\mathrm{loc}}\,\mathrm{d}Y \\ Nu=\dfrac{\overline{Nu}_{Ra}}{\overline{Nu}_{Ra=0}} \end{cases} \tag{5}$$

The volumetric flow rate is calculated as

$$\begin{cases} \dot V=-\displaystyle\int_{X=1} U_i\,\mathrm{d}Y \\ U_i=U_{X=1} \quad \text{if } U_{X=1}<0 \\ U_i=0 \quad \text{if } U_{X=1}>0 \end{cases} \tag{6}$$

The stream function is calculated from its definition as

$$U=-\frac{\partial\psi}{\partial Y},\qquad V=\frac{\partial\psi}{\partial X} \tag{7}$$

where ψ is zero on the solid surfaces and the streamlines are drawn by $\Delta\psi=(\psi_{\max}-\psi_{\min})/n$ with $n=$ number of increments.

4. Numerical technique

Following Chan and Tien [5], the computational domain was restricted to within the cavity. Hence, the boundary conditions are (see Fig. 1(b))

$$\begin{cases} \text{on solid surfaces} \quad U=0,\ V=0 \\ \text{on adiabatic walls} \quad \frac{\partial T}{\partial Y}=0 \\ \text{on the wall facing the opening} \quad q=\dfrac{\partial T}{\partial X} \\ \text{at the opening} \quad P=0,\ \dfrac{\partial V}{\partial X}=0, \\ \quad \dfrac{U}{X}=-\dfrac{\partial V}{\partial Y},\ \left(\dfrac{\partial T}{\partial X}\right)_{\mathrm{out}}=0,\ T_{\mathrm{in}}=0 \end{cases} \tag{8}$$

The numerical method used to solve Eqs. (1)–(4) is the SIMPLER (Semi-Implicite Method for Pressure Linked Equations Revised) algorithm formulated by Patankar [12]. The computer code based on the mathematical formulation discussed earlier and the SIMPLER method are validated for various cases published in the literature, the results of which are discussed elsewhere [11]. Uniform grid was used for all computations. Grid convergence was studied for a square cavity. Grid sizes from 16×16 to 60×60 were tried. Grid independence was achieved within 1.3 percent with a grid size of 30×30. Similar test were conducted with shallow cavities and the grid size was adjusted accordingly. For example, the grid size for 0.125 aspect ratio was 30×90 for $Ra\leqslant10^7$ and 45×90 for $Ra\geqslant10^8$. The execution time for a typical case with $A=1$, the grid size of 30×30, $Ra=10^6$ and for 680 iterations was 3 min 52 s and with $A=0.125$, the grid size 30×90 $Ra=10^6$ and for 3372 iterations was 32 min 59 s using a P.C. with 500 MHz clock speed. The accuracy control was carried out by the conservation of mass by setting its variation to less than 10^{-3}, on the pressure term by setting the variation of residues at 10^{-3}. In addition, the accuracy of computations was checked using the energy conservation within the system, by setting its variation to less than 10^{-4}.

4.1. Verification of results with square cavity

Isothermal side wall case studied earlier by Chan and Tien [3] by taking an extended computational domain was studied for verification of the code. Table 1 shows a comparison of the heat transfer *Nu* and the volumetric

Table 1
Comparison of results with a square cavity from [3] with enlarged computational domain and this study with computational domain within the cavity

Ra	*Nu* [3]	*Nu* this study	$\dot V$ [3]	$\dot V$ this study
10^3	1.07	1.320	1.95	2.631
10^4	3.41	3.570	8.02	9.325
10^5	7.69	7.811	21.10	22.650
10^6	15.00	15.230	47.30	47.018
10^7	28.60	30.707	96.00	94.248

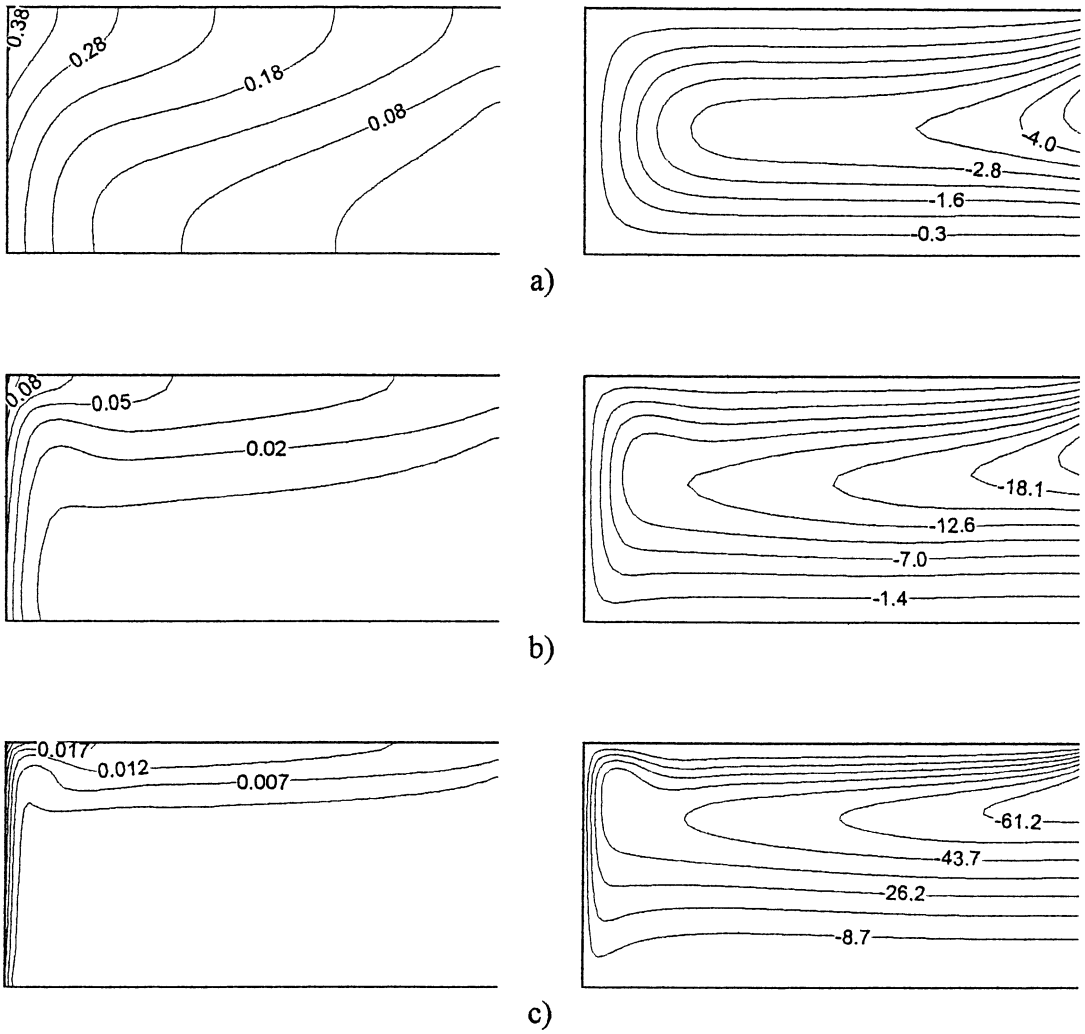

Fig. 2. Isotherms (on the left) and streamlines (on the right) for the case $A = 0.5$, $\varphi = 90°$ and various Ra numbers: (a) $Ra = 10^5$, (b) $Ra = 10^7$, and (c) $Ra = 10^9$.

flow rate through the cavity opening $\dot{V}$. The controlling parameters are $Pr = 1$, $A = 1$ and Ra from 10^3 to 10^7. It is seen that for $A = 1$ and $Pr = 1$, the deviations are 23.4% for Nusselt number and 34.92% for $\dot{V}$ at $Ra = 10^3$, they are respectively 4.69% and 16.27% at $Ra = 10^4$, 1.57% and 7.35% at $Ra = 10^5$, 1.52% and 0.60% at $Ra = 10^6$ and 7.37% and 1.8% at $Ra = 10^7$. The discrepancy at low Rayleigh numbers, particularly at conduction regime is explained by the fact that in the simplified computational method, the temperature at the opening is set at $T = 0$, which in turn increases the temperature gradient. At higher Rayleigh numbers, this effect disappears because a boundary layer type heat transfer and flow establishes, hence the agreement becomes better. At still higher Rayleigh numbers, the flow at the corners at the opening is with an angle when extended domain is considered and the simplified method is not able to simulate this situation. These discrepancies are the inherent shortcomings of the simplified method. Despite this, at the range of Rayleigh number considered in this study with constant heat flux, the approximation is acceptable.

5. Results and discussion

Flow and temperature fields, heat transfer and volumetric flow rate through the cavity are examined for ranges of the Rayleigh number from 10^3 to 10^{10}, the aspect ratio from 1 to 0.125 and for φ from 90° (heated wall at vertical position) to 45°. First the results are presented with $\varphi = 90°$ and later the effect of inclination is examined for φ from 90° to 45°. All results are with $Pr = 1$.

5.1. General observation

Isotherms and streamlines for $A = 0.5$ and 0.125 are presented respectively in Figs. 2(a)–(c) and 3(a)–(c) for $Ra = 10^5$, 10^7 and 10^9.

For $A = 0.5$, it was seen (not presented here) that at $Ra = 10^3$ and 10^4 the isotherms showed essentially a conduction dominated regime. At $Ra = 10^4$, they were distorted due to convective flow but the convection was however very weak. At $Ra = 10^5$, Fig. 2(a) shows that the isotherms are further

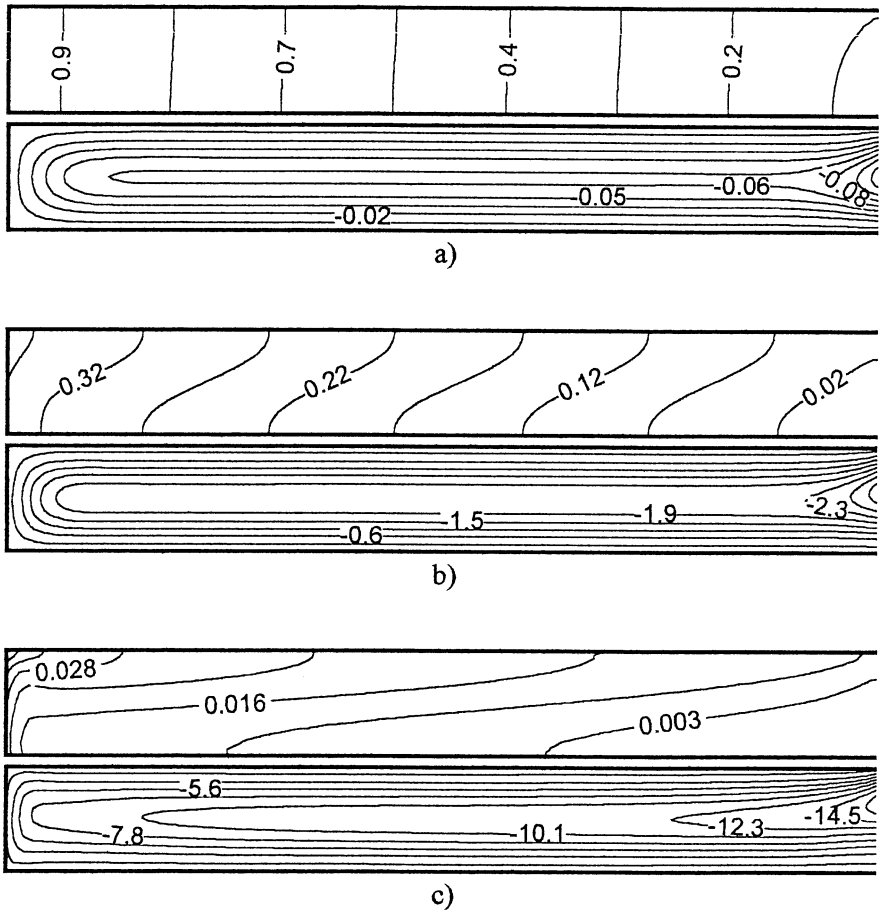

Fig. 3. Isotherms (on the left) and streamlines (on the right) for the case $A = 0.125$, $\varphi = 90°$ and various Ra numbers: (a) $Ra = 10^5$, (b) $Ra = 10^7$, and (c) $Ra = 10^9$.

distorted by the flow, the temperature gradient is almost constant especially at the lower part of the cavity where the fluid flows following the bottom wall. The convection has increased and it is an equally dominant regime. The streamlines show a parallel flow with a core at the center except at the opening. As Ra is increased further to 10^7, the isotherms in Fig. 2(b) show that the cold fluid penetrates right to the heated wall, where steep temperature gradients exist. The flow becomes similar to boundary layer type and the core disappears. At $Ra = 10^9$, Fig. 2(c) shows that heat transfer and flow is a boundary layer type, the cold fluid penetrates to the heated wall and the convection is rigorous. Flow of the hot fluid from the opening is choked, as a result of which the fluid velocities are increased.

For $A = 0.125$ and low Rayleigh numbers at 10^3–10^4 (not shown here) the heat transfer mode was essentially by conduction, with constant temperature gradients and parallel flow. This situation has continued also at $Ra = 10^5$. In Fig. 3(a), the isotherms show a conduction dominated regime. The convective flow in the shallow cavity is very weak as it can be noticed in the lower part showing the streamlines. The temperature field is only slightly distorted by the convective flow. The temperature gradient is nearly constant along the cavity, especially near the opening, which is responsible for the circulation of the fluid in the cavity. The streamlines show a parallel flow, which is from the opening to the heated wall where it turns around. It flows counter current to the incoming fluid, which cools it down, resulting in the isotherms observed. As Ra increases to 10^7 (Fig. 3(b)), the heat transfer mode becomes convective and isotherms are noticeably distorted, although a constant temperature gradient exists along the cavity. The flow is essentially similar but a boundary layer heat transfer and flow is noticed especially near the vertical wall. A core region also exits between two parallel flows. At $Ra = 10^9$ the flow regime is clearly convective and the strength of the circulation increased. A boundary layer type heat transfer and flow is observed. The flow at the exit is further choked. At $Ra = 10^{10}$ the isotherms showed (not presented here) that the cold fluid penetrated all the way through the cavity until it reached the heated wall and a boundary layer type flow existed. It should be noted that the flow was unicellular in all cases considered in this study.

5.2. Temperature and velocity profiles

Non-dimensional temperature profiles on the heated wall, at the opening and the horizontal velocity profile at the

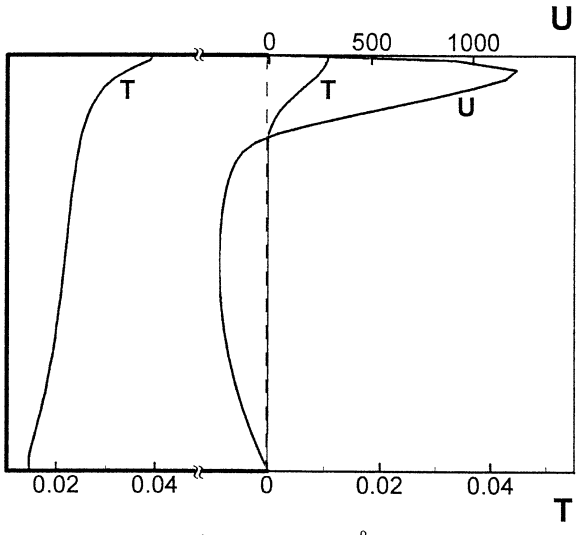

a) A=0.5; Ra=10^9

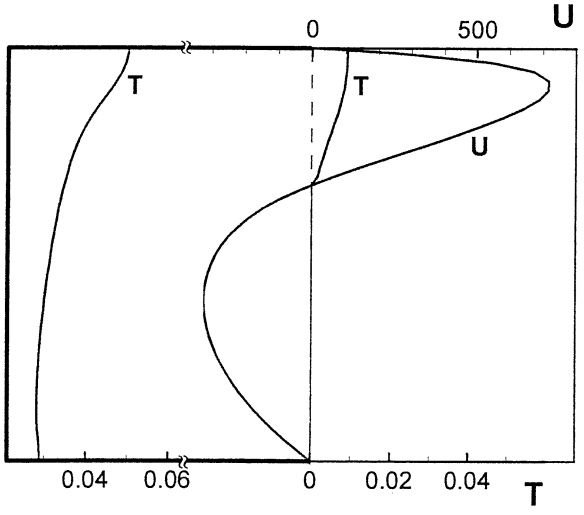

b) A=0.125; Ra=10^9

Fig. 4. Non-dimensional temperature profiles on the heated wall and at the opening and the horizontal velocity profile at the opening for $\varphi = 90°$ at $Ra = 10^9$: (a) $A = 0.5$, and (b) $A = 0.125$.

opening at $Ra = 10^9$ are shown in Fig. 4(a) and (b) for $A = 0.5$ and 0.125, respectively. It is seen in both cases that the heated wall temperature follows a non-linear variation, low near the bottom and high at the top. The cold fluid entering the cavity is heated along the wall, cooling it more effectively at lower elevations. As the heated fluid convects along the wall, the wall temperature also increases. The temperature profile at the opening shows that the temperature is $T = 0$ at the lower portion where the fluid enters the cavity and hot fluid exits at the remaining upper portion. The outgoing flow occupies 19.3% of the opening with $A = 0.5$ while 33.3% with $A = 0.125$. This is related to the volume flow rate for each case and is consistent with the observation made with streamlines in Figs. 2 and 3.

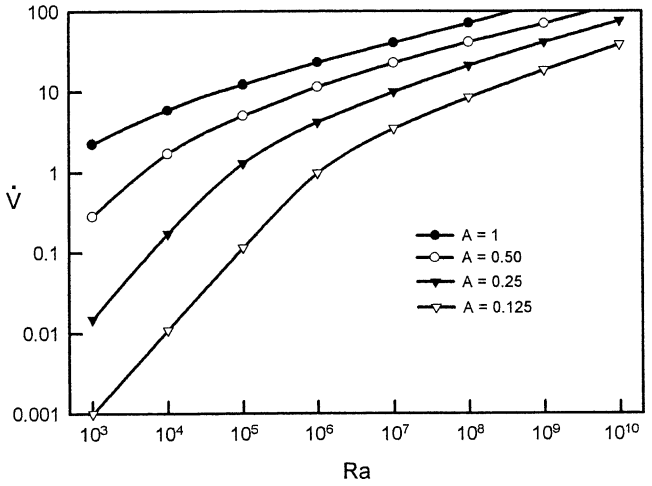

Fig. 5. Volumetric flow rate as a function of Rayleigh number with the aspect ratio as a parameter for the case $\varphi = 90°$.

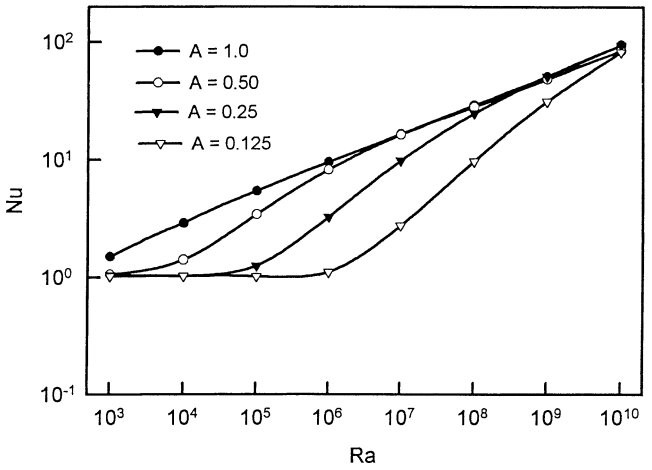

Fig. 6. Heat transfer (normalized Nusselt number) as a function of Rayleigh number with the aspect ratio as a parameter for the case $\varphi = 90°$.

5.3. Volumetric flow rate

Non-dimensional volumetric flow rate in and out the cavity, $\dot{V}$ has been calculated using Eq. (6) and shown in Fig. 5 as a function of *Ra* with *A* as a parameter. As expected, $\dot{V}$ is an increasing function of *Ra* and *A*. At a given *Ra*, shallower the cavity, smaller becomes the volumetric flow rate. The volumetric flow rates approach asymptotic values; the variation of $\dot{V}$ as a function of *Ra* is $\dot{V} \sim Ra^{0.253}$. For a flat plate with constant heat flux, the volumetric flow rate varies with *Ra* to the power of 0.25 [13].

5.4. Heat transfer

Heat transfer reduced as normalized Nusselt number, *Nu* as a function of Rayleigh number, *Ra* is shown in Fig. 6 where the aspect ratio, *A* is a parameter. Nusselt number is calculated using Eq. (5), which is equal to unity for purely conduction heat transfer. Modified Rayleigh number is defined as in the nomenclature with q'' and length scale

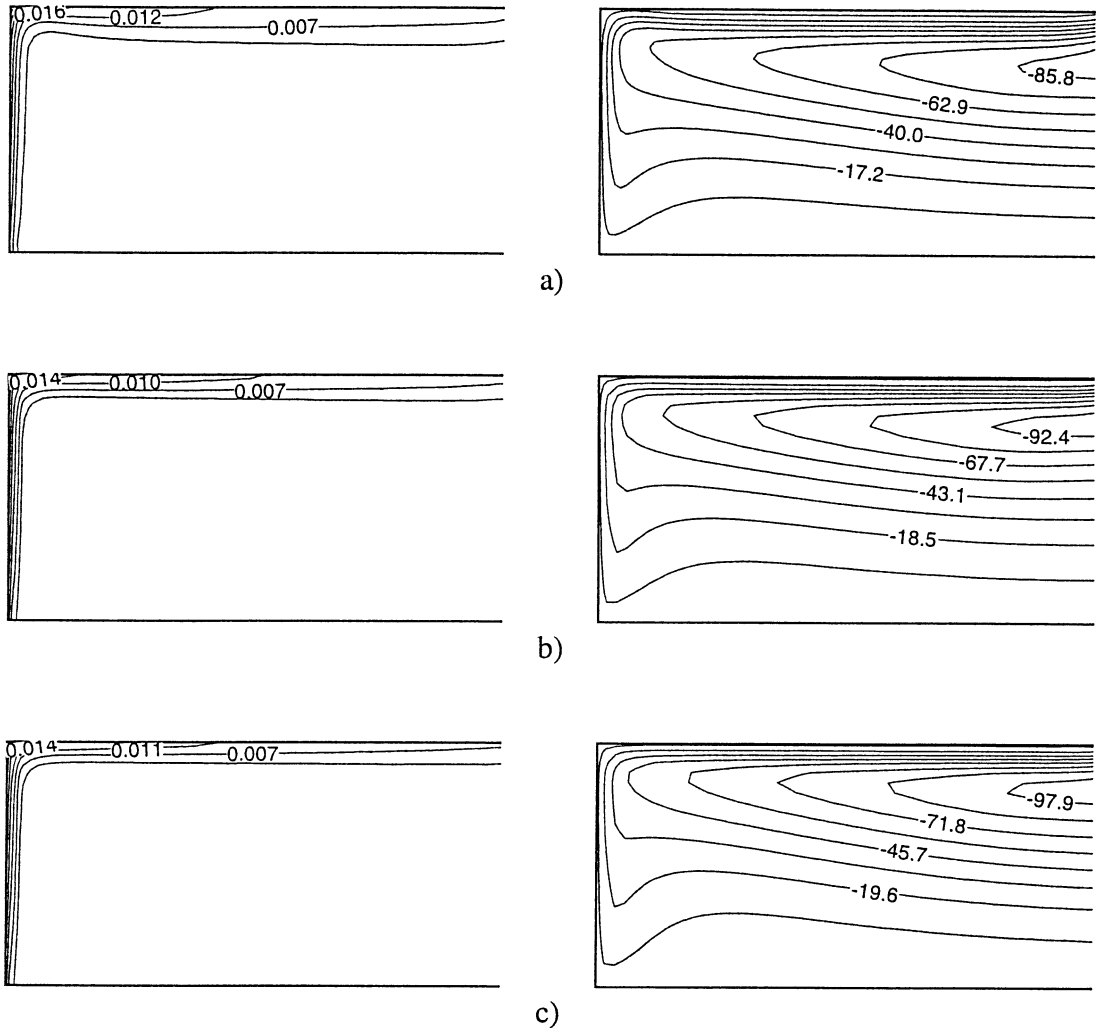

Fig. 7. Isotherms (on the left) and streamlines (on the right) for the case $A = 0.5$, $Ra = 10^9$ and various inclination angles: (a) $\varphi = 75°$, (b) $\varphi = 60°$, and (c) $\varphi = 45°$.

L. At low Rayleigh numbers, Nusselt number is close to unity. For square cavity, Nu is close to unity at $Ra = 10^3$; as Rayleigh increases, convection increases and heat transfer becomes dominated by convection. It approaches asymptotic values at high Rayleigh numbers as heat transfer becomes mainly a boundary layer type of flow. Nu varies as a function of Ra to the power of 0.242, which is independent of the aspect ratio. For a vertical flat plate with constant heat flux, Nu varies with Ra to the power of 0.25 [13], which is close to the asymptotic value found for shallow cavities in this study. For shallow cavities, Nu is equal to unity at $Ra = 10^3$; as the aspect ratio decreases towards $A = 0.125$, Nusselt number stays close to unity at higher Rayleigh numbers until $Ra = 10^6$. As observed with Figs. 2 and 3, the flow goes through a transition and convection becomes dominant at higher Rayleigh numbers. This transition is delayed as the aspect ratio is decreased. It is seen also that for longer cavities, the asymptotic behavior is delayed to still higher Rayleigh numbers. For example, for $A = 0.125$, the asymptotic values are reached beyond $Ra = 10^{10}$.

5.5. *Effect of inclination angle*

The effect of inclination is examined for φ from 90 to 45° and with $A = 0.5$ and 0.25, covering practical cases in solar collectors and other applications. Isotherms and streamlines for a typical case with $A = 0.5$ and $Ra = 10^9$ are presented in Fig. 7 for 75°, 60° and 45° inclinations of the heated wall from the horizontal. The case with $\varphi = 90°$ is presented in Fig. 2(c). Isotherms and streamlines show that as the inclination angle of the heated plate decreases, the velocity gradient increases at upper adiabatic wall, the strength of the circulation increases. In fact streamlines on the right show that $|\Psi|$ increases considerably making the convection more rigorous when the heated wall is inclined further. Flow of the hot fluid from the opening is choked as the inclination is decreased, as a result of which the fluid

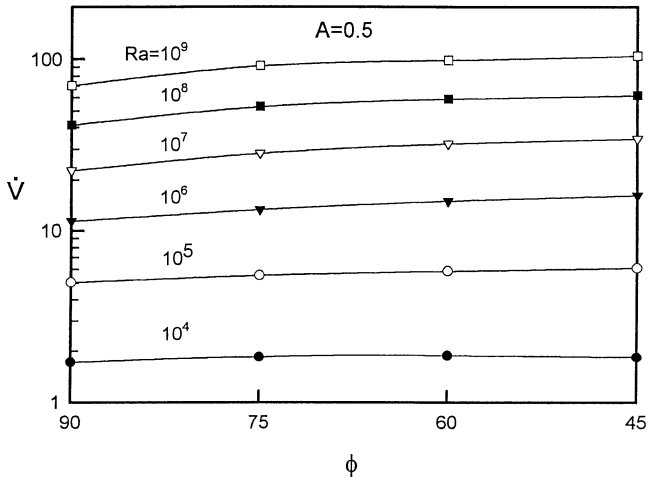

Fig. 8. Volumetric flow rate as a function of the inclination angle for various Rayleigh numbers.

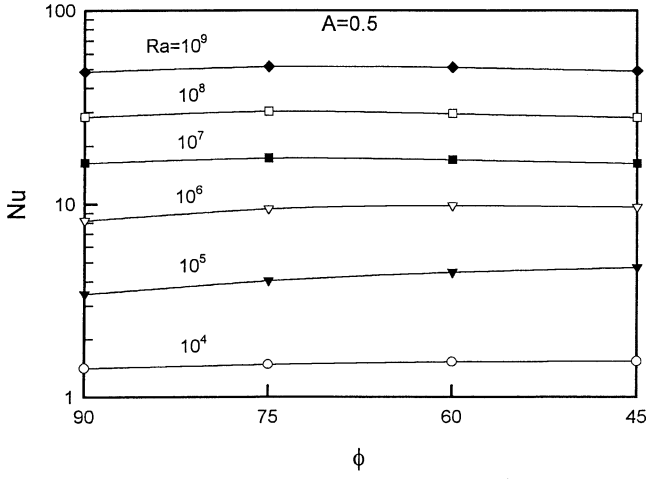

Fig. 9. Heat transfer (normalized Nusselt number) as a function of the inclination angle for various Rayleigh numbers.

velocities are increased. Isotherms show that the temperature gradient is also similarly affected. The temperature gradients are clearly increased as the opening faces more and more upward. Therefore, as expected, the volumetric flow rate and heat transfer should increase with decreasing inclination angle of the heated plate. Similar observations were made with $A = 0.25$ for the same inclination angles (not shown in figures) with strength of convection relatively more vigorous than with $A = 0.5$.

For $A = 0.5$, volumetric flow rate as a function of inclination angle is shown in Fig. 8 with *Ra* as a parameter. It is seen that the volumetric flow rate increases with decreasing inclination angle of the heated wall or when the opening faces upward from the horizontal. It is noted that $(90° - \varphi)$ is the slope of the open cavity as show in Fig. 1(b). The relative increase varies from about 9% to 52%, the latter corresponding to $\varphi = 45°$ at $Ra = 10^7$ for this case. For $A = 0.25$, it was seen (not shown in figures) that a similar observation could be made. The variation of the relative increase was however more discernible, from 6% to 76%, the latter corresponding to $\varphi = 45°$ at $Ra = 10^9$.

Heat transfer for the case $A = 0.5$ is presented in Fig. 9 where *Nu* is plotted as a function of φ with *Ra* as a parameter. Similar to the observation made with the volumetric flow rate, the heat transfer increases with decreasing inclination of the heated plate. The variation of *Nu* with φ is from about 8% to 36%, which is at $\varphi = 45°$. Similar observations were made with $A = 0.25$, but the variation of the relative increase was up to 54%. It is seen that contrary to the findings by Mohamad [4] for the case of isothermal wall, the inclination angle is a strong parameter in this case.

6. Conclusions

Laminar natural convection in inclined open shallow cavities has been numerically studied for the case of constant heat flux at the end wall and adiabatic at the walls perpendicular to the heated wall. Equations of mass, momentum and energy have been solved using constant properties and Boussinesq approximation. The computation domain has been restricted to the cavity and approximate boundary conditions at the opening have been assumed. Isotherms, streamlines, and temperature and velocity profiles have been produced; the volumetric flow rate in and out the cavity and heat transfer as a function of Rayleigh number and the aspect ratio have been obtained. It is found that volumetric flow rate and heat transfer are increasing functions of the aspect ratio and Rayleigh number. Heat transfer for a given aspect ratio has an asymptotic behavior. Asymptotic values are reached as Rayleigh increased. For shallower cavities, this transition is delayed at higher Rayleigh numbers. It is also found that the inclination angle of the heated plate is an important parameter affecting volumetric flow rate and the heat transfer.

Acknowledgements

Financial support by Natural Sciences and Engineering Research Council of Canada is acknowledged.

References

[1] P. Le Quere, J.A.C. Humphrey, F.S. Sherman, Numerical calculation of thermally driven two-dimensional unsteady laminar flow in cavities of rectangular cross section, Numer. Heat Transfer 4 (1981) 249–283.
[2] F. Penot, Numerical calculation of two-dimensional natural convection in isothermal open cavities, Numer. Heat Transfer 5 (1982) 421–437.
[3] Y.L. Chan, C.L. Tien, A numerical study of two-dimensional natural convection in square open cavities, Numer. Heat Transfer 8 (1985) 65–80.
[4] A.A. Mohamad, Natural convection in open cavities and slots, Numer. Heat Transfer 27 (1995) 705–716.
[5] Y.L. Chan, C.L. Tien, A numerical study of two-dimensional laminar natural convection in shallow open cavities, Internat. Heat Mass Transfer 28 (3) (1985) 603–612.

[6] V. Sernas, I. Kyriakides, Natural convection in an open cavity, in: Proc. the Seventh Internat. Heat Transfer Conf., Munich, Vol. 2, 1982, pp. 275–286.

[7] C.F. Hess, R.H. Henze, Experimental investigation of natural convection losses from open cavities, J. Heat Transfer 106 (1984) 333–338.

[8] S.S. Cha, K.J. Choi, An interferometric investigation of open cavity natural convection heat transfer, Exp. Heat Transfer 2 (1989) 27–40.

[9] Y.L. Chan, C.L. Tien, Laminar natural convection in shallow open cavities, J. Heat Transfer 108 (1986) 305–309.

[10] E. Bilgen, Passive solar massive wall systems with fins attached on the heated wall and without glazing, J. Solar Energy Engrg. xx (2000).

[11] Z.-G. Du, E. Bilgen, Natural convection in vertical cavities with internal heat generating porous medium, Waerme- und Stoffuebertragung 27 (1992) 149–155.

[12] S.V. Patankar, Numerical Heat Transfer and Fluid Flow, Hemisphere, New York, 1980.

[13] E.M. Sparrow, J.L. Gregg, Laminar free convection from a vertical plate with uniform surface heat flux, Trans. ASME 78 (1956) 435–440.